186 *Chem. Mater.* **2010,** *22,* 186–196
DOI:10.1021/cm902800y

CHEMISTRY OF MATERIALS
Article

Facile Scalable Synthesis of Rectorites

Michael W. Möller,[†] Dunja Hirsemann,[†] Frank Haarmann,[‡] Jürgen Senker,[†] and Josef Breu*,[†]

[†]*Lehrstuhl für Anorganische Chemie I, Universität Bayreuth, D-95440 Bayreuth, Germany and* [‡]*Institut für Anorganische Chemie, RWTH Aachen, D-52074 Aachen, Germany*

Received September 8, 2009. Revised Manuscript Received November 16, 2009

Using a synthetic Na-fluorohectorite ($[Na_{0.5}]^{inter}[Mg_{2.5}Li_{0.5}]^{oct}[Si_4]^{tet}O_{10}F_2$), mixed-cation heterostructures with an alternating interstratification pattern are formed under appropriate conditions via simple cation-exchange reactions. The most important requirement for the spontaneous formation of these ordered mixed-layer structures is a high degree of charge homogeneity of the smectite. The partial exchange of cations with largely different hydration enthalpies (Na^+ by K^+) results in the regular interstratification of hydrated (d = 12.4 Å) and nonhydrated (d = 10.0 Å) interlayers at 40% relative humidity (RH). By combining analytical methods that are sensitive to either hydrated or collapsed interlayers (selective cation exchange, hydrosorption isotherms, and ^{23}Na MAS NMR spectroscopy), we proposed a novel mechanism that is centered at the interlayers and does not require polar lamellae, as suggested in the literature for rectorite formation. Upon formation of the regular interstratification, the charge density of the interlayers changes from homogeneous to alternating between interlayers in the stacking direction. This simple redistribution of exchangeable interlayer cations is facile and rapid. The cation exchange capacity (CEC) of the collapsed interlayers is higher than the average CEC, while the CEC of the hydrated interlayers will be correspondingly lower. The local CEC of these interlayers deviates by ∼18%−28% from the average CEC, as calculated independently from ion-exchange experiments and hydrosorption measurements. Moreover, this alternating differentiation of the interlayer cation concentration seems to be driven by thermodynamics. Even a mixture of homocationic Na-hectorite and K-hectorite slowly converts to a regularly interstratified material when immersed in water. After the interlayers are differentiated, they may be selectively manipulated, creating dual functional materials, where distinct nanoreactors are separated by a 1-nm-thick insulating lamellae and are arranged in a regular manner.

1. Introduction

The chemical and physical properties of many layered materials can easily be tuned by intercalation. Consequently, a plethora of applications in various fields of current materials chemistry (e.g., for sensor or electrode materials, adsorbents, catalysts, fillers, and additives) has been examined.[1−10] Smectites are often singled out among layered materials, because the solvation or complexation of their interlayer cations increases their intracrystalline reactivity.[11,12] Moreover, the silicate lamellae that build 2:1 layered silicates like smectites represent two-dimensional polyanions. Consequently, the Coulombic interaction with the interlayer cations tends to minimize the average basal spacings. Therefore, mixed interlayer cations of different sizes will be segregated into different interlayers. The different interlayers of such interstratified materials may be stacked in an ordered (regular) or random fashion.

The most trivial intracrystalline reaction, the hydration of interlayer cations, which is also referred to as swelling, has been extensively investigated over decades[13−17] and

*Author to whom correspondence should be addressed. Tel.: (+49) 921-552530. Fax: (+49) 921-552788. E-mail: josef.breu@uni-bayreuth.de.

(1) Fukuda, K.; Akatsuka, K.; Ebina, Y.; Ma, R.; Takada, K.; Nakai, I.; Sasaki, T. *ACS Nano* **2008**, *2*, 1689–1695.
(2) Behrens, M.; Wontcheu, J.; Kiebach, R.; Bensch, W. *Chem.—Eur. J.* **2008**, *14*, 5021–5029.
(3) Behrens, M.; Riemenschneider, O.; Bensch, W.; Indris, S.; Wilkening, M.; Heitjans, P. *Chem. Mater.* **2006**, *18*, 1569–1576.
(4) Lotsch, B. V.; Ozin, G. A. *ACS Nano* **2008**, *2*, 2065–2074.
(5) Tsapatsis, M.; Maheshwari, S. *Angew. Chem., Int. Ed.* **2008**, *47*, 4262–4263.
(6) Stöcker, M.; Seidl, W.; Seyfarth, L.; Senker, J.; Breu, J. *Chem. Commun.* **2008**, 629–631.
(7) Morel, J. P.; Marry, V.; Turq, P.; Morel-Desrosiers, N. *J. Mater. Chem.* **2007**, *17*, 2812–2817.
(8) Mariychuk, R.; Baumgartner, A.; Wagner, F. E.; Lerf, A.; Dubbe, A.; Moos, R.; Breu, J. *Chem. Mater.* **2007**, *19*, 5377–5387.
(9) Baumgartner, A.; Sattler, K.; Thun, J.; Breu, J. *Angew. Chem., Int. Ed.* **2008**, *47*, 1640–1644.
(10) Sanchez, C.; Julian, B.; Belleville, P.; Popall, M. *J. Mater. Chem.* **2005**, *15*, 3559–3592.
(11) Bergaya, F.; Theng, B. K. G.; Lagaly, G. *Handbook of Clay Science*; Elsevier: Amsterdam, 2006.
(12) Konta, J. *Appl. Clay Sci.* **1995**, *10*, 275–335.
(13) Marry, V.; Malikova, N.; Cadene, A.; Dubois, E.; Durand-Vidal, S.; Turq, P.; Breu, J.; Longeville, S.; Zanotti, J. M. *J. Phys. Condens. Mat.* **2008**, *20*, 4205.
(14) Malikova, N.; Cadene, A.; Dubois, E.; Marry, V.; Durand-Vidal, S.; Turq, P.; Breu, J.; Longeville, S.; Zanotti, J. M. *J. Phys. Chem. C* **2007**, *111*, 17603–17611.
(15) Tenorio, R. P.; Alme, L. R.; Engelsberg, M.; Fossum, J. O.; Hallwass, F. *J. Phys. Chem. C* **2008**, *112*, 575–580.
(16) da Silva, G. J.; Fossum, J. O.; DiMasi, E.; Maloy, K. J. *Phys. Rev. B* **2003**, *6709*, 4114.
(17) da Silva, G. J.; Fossum, J. O.; DiMasi, E.; Maloy, K. J.; Lutnaes, S. B. *Phys. Rev. E* **2002**, *6601*, 1303.

Published on Web 12/03/2009
© 2009 American Chemical Society

has been recently reviewed by Ferrage et al.[18] Numerous models have been proposed to explain this phenomenon, and different coordinating water molecule structures within the interlayer have been suggested. Since they are generated under relatively mild conditions, the intracrystalline reactivity of natural clay minerals is nonuniform and often masked by the immanent charge heterogeneities. Since electrostatics plays an important role in the cation exchange processes of clay minerals, these local charge fluctuations alter the exchange properties over various length scales. Most analytical methods such as powder X-ray diffraction (PXRD) only allow for the observation of average values, and localized swelling data are difficult to obtain. Contrary to natural smectites, hectorites synthesized from the melt exhibit a highly homogeneous charge density, which helps to overcome these difficulties. Moreover, charge homogeneity fosters the formation of regular interstratification when performing a partial exchange of two interlayer cations, which differ in size or hydration at a given relative humidity (RH).[9,19] However, the charge heterogeneity of natural smectites always triggers random interstratifications.

Using these regular interstratified materials, two distinct nanoreactors separated by a 1-nm-thick insulating lamellae are arranged in a regular manner, which provides several advantages, such as the possibility for an electronic or energetic communication between the two adjacent reaction spaces. Pinnavaia described the formation of a mixed inorganic−organic layered material using cationic amphiphiles[20−22] and explored numerous potential applications of these materials. A rare representative of a natural regular interstratified material—rectorite—was recently proven to be advantageous over simple smectites when used as an inorganic reinforcing filler in polymer−layered silicate nanocomposites.[23−25]

In addition to material science aspects, there is a great deal of interest in these mixed-layer minerals, because they have been attributed to playing a role in the formation of life as simple inorganic prebiotic RNA.[26−28] Additionally, and largely unnoticed by the material science community, interstratified materials are of interest to the geochemistry community and oil industry, because illite−smectite interstratified clay minerals are ubiquitous in sedimentary basins and are related to the maturation, migration, and trapping of hydrocarbons.[29]

Despite this broad interdisciplinary interest in regular interstratified materials, their hypothesized structures are controversial. Two competing models have been proposed, each with profoundly different consequences for describing the diagenetic processes. Attempts to experimentally clarify the mechanism of formation or specify the structure in natural regularly interstratified clays have been prone to failure due to small crystal sizes, complex composition, and turbostratic stacking (translational and/or rotational disorder between adjacent lamellae in the stack). To elucidate the formation mechanism of regular interstratified materials, synthetic model substances must be used. Once the mechanism is established, robust and versatile large-scale synthesis may be established, which is needed for material science applications.

Applying a synthetic fluorohectorite allows us to conduct a detailed analysis of the composition, structure, and local environment of interlayer cations and enables us to propose a novel mechanism for the formation of ordered mixed-layer materials that, thus far, has been overlooked. Furthermore, we succeeded in an inexpensive and simple production of an ordered mixed-layer material that allows for further modification by intercalation while preserving the desirable alternating structural pattern.

2. Experimental Methods

The clay used in this study was a synthetic Na-fluorohectorite (Na-Hec) that was prepared in a closed molybdenum crucible via melt synthesis according to a published procedure.[19] The chemical composition of the synthesized Na-Hec was initially $[Na_{0.5}]^{inter}[Mg_{2.5}Li_{0.5}]^{oct}[Si_4]^{tet}O_{10}F_2$ (formula unit), but when washed with water, ~14% of the total Na^+ is released due to hydrolysis of the Na-silanolate groups located at the edges of the lamellae. As a result, the effective layer charge (x) is slightly less than 0.5. For both the initial and washed Na-Hec, the cation exchange capacity (CEC), as determined by the $[Cu(trien)]^{2+}$ method described by Lagaly[30], was 113 and 97 mequiv/100 g, respectively. $[Cu(trien)]^{2+}$ was prepared from $CuSO_4$ (99.99+%) and triethylene tetramine (>97%, trien) was purchased from Sigma Aldrich. Samples were filtered using Whatman Anotop 0.1-μm syringe filters prior to the photometric measurements.

Partial exchange of $[K]^{inter}$ for $[Na]^{inter}$ was performed in glass vessels with screw caps. Typically, 500 mg of unwashed, dry Na-Hec was first immersed in water to preswell the fluorohectorite. The amount of water added was adjusted so that, upon addition of the various volumes of aqueous KCl (p.a. quality, from Grüssing GmbH) (2 g/L) needed to achieve the desired degree of exchange, a constant final concentration of 0.02 M in KCl was achieved for all suspensions. For example, 501.04 mg of Na-Hec was immersed in 4.07 mL of water and then 12.156 mL of the KCl solution was added for the 50% exchange. The amount of K^+ added is normalized to the theoretical stoichiometry, assuming a molar mass of 386.07 g/mol for the unwashed Na-Hec, and the Na^+ content was 0.5 $mol/mol_{Na\text{-}Hec}$. The solutions were thoroughly mixed in

(18) Ferrage, E.; Lanson, B.; Malikova, N.; Plancon, A.; Sakharov, B. A.; Drits, V. A. *Chem. Mater.* **2005**, *17*, 3499–3512.
(19) Breu, J.; Seidl, W.; Stoll, A. J.; Lange, K. G.; Probst, T. U. *Chem. Mater.* **2001**, *13*, 4213–4220.
(20) Pinnavaia, T. J.; Ijdo, W. L.; Lee, T. *Adv. Mater.* **1996**, *8*, 79–83.
(21) Pinnavaia, T. J.; Ijdo, W. L. *J. Solid State Chem.* **1998**, *139*, 281–289.
(22) Ijdo, W. L.; Pinnavaia, T. J. *Chem. Mater.* **1999**, *11*, 3227–3231.
(23) Wang, X. Y.; Du, Y. M.; Luo, J. W.; Yang, J. H.; Wang, W. P.; Kennedy, J. F. *Carbohyd. Polym.* **2009**, *77*, 449–456.
(24) Liu, J. H.; Wang, A. Q. *J. Appl. Polym. Sci.* **2008**, *110*, 678–686.
(25) Yu, J. H.; Cui, G. J.; Wei, M.; Huang, J. *J. Appl. Polym. Sci.* **2007**, *104*, 3367–3377.
(26) Cairns-Smith, A. G. *Chem.—Eur. J.* **2008**, *14*, 3830–3839.
(27) Greenwell, H. C.; Coveney, P. V. *Origins Life Evol. B* **2006**, *36*, 13–37.
(28) Hartman, H. *Origins Life Evol. B* **1998**, *28*, 515–521.
(29) Stixrude, L.; Peacor, D. R. *Nature* **2002**, *420*, 165–168.
(30) Lagaly, G.; Bergaya, F.; Ammann, L. *Clay Miner.* **2005**, *40*, 441–453.

an overhead shaker at room temperature (RT). The resulting heterocationic fluorohectorites were repeatedly washed with deionized water until the test for Cl^- using $AgNO_3$ was negative. All supernatants were collected, filtered, and analyzed for Na^+ and K^+ using a Varian SpectrAA-100 atomic absorption spectrometer. The heterocationic hectorites were separated from the suspensions by centrifugation and then freeze-dried. For the AAS analyses of the solid samples, 20-mg samples were weighed into a clean 150-ml Teflon flask. After adding 1.5 mL of 30 wt % HCl (Merck), 0.5 mL of 85 wt % H_3PO_4, 0.5 mL of 65 wt % HNO_3 (Merck), and 1 mL of 48 wt % HBF_4 (Merck), the samples were digested in a MLS 1200 Mega microwave digestion apparatus for 6.5 min and heated at 600 W (MLS GmbH, Mikrowellen-Labor-Systeme, Leutkirch, Germany). The closed sample containers were cooled to RT, and the clear solution was diluted to 100 mL in a volumetric flask prior to analysis.

The $[Na]^{inter} \rightarrow [Cu(trien)]^{inter}$ exchange of the ordered Na:K-Hec was conducted at RT. A freeze-dried portion of Na:K-Hec (250 mg) was suspended in ~10 mL of deionized water. Then, 4 mL of a freshly prepared 50 mM solution of $Cu(trien)Cl_2$ and more deionized water was added to bring the total volume to 25 mL. After shaking for 10 min, the hectorite was centrifuged and washed until the supernatant was colorless.

Textured PXRD samples were prepared by quickly drying a few drops of the aqueous fluorohectorite suspensions on a microscope slide (Menzel Gläser) at 120 °C in a furnace. The samples were equilibrated at ambient conditions (RT, 40%−55% RH) prior to measurement on a Panalytical XPERT-PRO diffractometer with a X'Celerator Scientific detector using nickel-filtered Cu Kα radiation (40 kV, 40 mA). The use of a highly (00*l*)-textured sample in Bragg−Brentano-geometry (reflection mode) simplifies the analysis since basal reflections are amplified while *hk*-bands fade or even vanish.

Hydrosorption measurements were performed with a Quantachrome Hydrosorb-1000 at 25 °C and relative water vapor pressures ranging from 0.05 to 0.95. Samples were dehydrated at 300 °C for 1 h in vacuo prior to measurement.

The solid-state ^{23}Na NMR spectra were obtained under magic angle spinning (MAS) conditions with a Bruker Avance II 300 spectrometer operating at a resonance frequency ν_0 of 79.4049 MHz. All measurements were performed using a standard double-resonance 4-mm MAS probe (Bruker) at RT. The freeze-dried samples were held in zirconia rotors and spun at 12.5 kHz. The pulse length was set to 1.7 μs, optimized with respect to the maximal intensity of Na-Hec at 45% RH, giving a recycling delay of 3.5 s. The peak positions are referenced with respect to 1 M NaCl solution. The samples were measured at 0% RH and 45% RH. The samples at 0% RH were heated at 180 °C in a fine vacuum at least for 3 days and kept under dry argon. The samples at 45% RH were equilibrated for at least 3 days at constant RH. The completely exchanged K-Hec* was prepared from the regularly interstratified Na:K-Hec by the addition of 1 M KCl solution in excess. After vigorous manual shaking for 1 min, the vessel was placed into an overhead shaker for 2 days at RT. Since some aggregates were present, the dispersion was sonicated in an ultrasonic bath for 5 min and the reaction was continued for another 3 days. The KCl solution was renewed once during this time. The fluorohectorite was finally washed with deionized water until the test for Cl^- using $AgNO_3$ was negative.

The calculations of the quadrupole coupling tensor of Na^+ (electric-field gradient) were performed with CASTEP (MS Modeling 4.0 package by Accelerys). Single-point calculations were performed with the unit cell and atomic coordinates taken from taeniolite,[31] $[K_{1.0}]^{inter}[Mg_{2.0}Li_{1.0}]^{oct}[Si_4]^{tet}O_{10}F_2$. The symmetry was reduced to P1; however, the stacking mode was fixed to 1 M with hexagonal cavities encompassing the interlayer cations arranged exactly opposite. Thus, no rotational or translational planar defects were allowed for the DFT calculations. To circumvent a mixed occupancy of the octahedral sites by Li and Mg, all octahedral positions were filled with Mg, which carries a reduced formal charge of $^5/_3$ instead of 2, to generate a layer charge of 1 per formula unit (pfu). The two symmetrically independent interlayer cation positions in P1 were filled with 1 K^+ and 1 Na^+, respectively. The calculation of the exchange correlation energies was implemented using the Perdew−Burke−Ernzerhof (PBE) functional. The "on the fly" pseudopotentials were used with a kinetic energy cutoff for the planewave basis set of 610 eV. The sampling was accomplished over 15 *k*-points.

3. Results and Discussion

3.1. Incremental Cation Exchange. For natural and some synthetic materials produced at low temperatures, it has been established that the charge density is rather heterogeneous; hence, the intracrystalline reactivity is expected to be nonuniform.[32−34] With clays such as these, the partial cation exchange with interlayer cations of different sizes produces heterocationic clays where the different cations usually segregate into different interlamellar spaces. However, due to the heterogeneity, the different basal spacings are randomly stacked and statistically interstratified materials are obtained. Monte Carlo simulations of the order−disorder behavior of octahedral phyllosilicate sheets confirm that, for most compositions, the cations are short-range-ordered; that is, the layers inherently exhibit charge heterogeneities at low temperatures.[35] Although this short-range order has been found to be heavily dependent on the nature of the cation, temperatures exceeding 1000 K are often necessary to achieve a disordered solid solution with a homogeneous charge density. The synthetic Na-Hec used in this study was synthesized from melt and indeed shows a uniform intracrystalline reactivity, as determined by various intercalation reactions.[13,14,19,36]

Given a layer charge of 0.5 pfu, the Na-Hec forms a monolayer hydrate with a *d*-value of 12.3 Å under ambient conditions (RT, 40%−55% RH), whereas the correspondent K-Hec collapses to 10.0 Å (see Figure S1 in the Supporting Information). This is mainly attributed to the difference in hydration enthalpy, which is −406 kJ/mol for Na^+ and only −322 kJ/mol for K^+. Thus, upon partial cation exchange with K^+, a situation will be encountered

(31) Toraya, H.; Iwai, S.; Marumo, F.; Hirao, M. *Z. Kristallogr.* **1977**, *146*, 73–83.
(32) Decarreau, A.; Grauby, O.; Petit, S. *Appl. Clay Sci.* **1992**, *7*, 147–167.
(33) Muller, F.; Besson, G.; Manceau, A.; Drits, V. A. *Phys. Chem. Miner.* **1997**, *24*, 159–166.
(34) Lagaly, G. *Clays Controlling the Environment*; Churchman, G. J., Fitzpatrick, R. W., Eggleton, R. A., Eds.; CSIRO Publishing: Melbourne, Australia, 1995; pp 137−144.
(35) Palin, E. J.; Dove, M. T.; Hernandez-Laguna, A.; Sainz-Diaz, C. I. *Am. Mineral.* **2004**, *89*, 164–175.
(36) Breu, J.; Stoll, A.; Lange, K. G.; Probst, T. *Phys. Chem. Chem. Phys.* **2001**, *3*, 1232–1235.

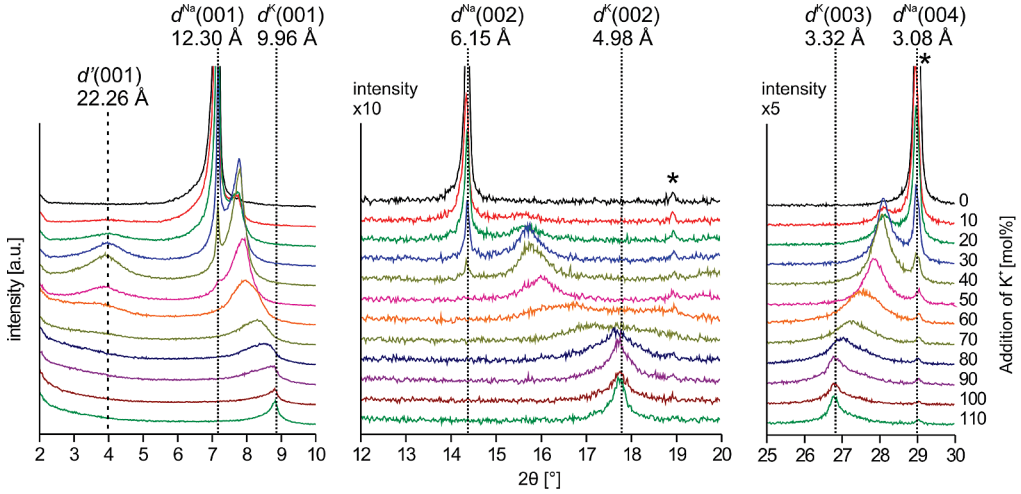

Figure 1. Details of the PXRD patterns with respect to the added amount of K^+. Reflections of a trace impurity of protoamphibole are marked with an asterisk.

in which two differently sized interlayer cations, hydrated Na^+ and nonhydrated K^+, segregate into different interlayer spaces.

It is also noteworthy that, since we are dealing with a hectorite-type clay, the permanent negative charge of the silicate lamella is derived exclusively from isomorphous substitution within the octahedral sheet, and thus, the charge distribution perpendicular to the lamellae is symmetrical by definition. Nevertheless, upon partial cation exchange, we observe a strong tendency for the formation of regular interstratifications with this type of clay. Upon incremental addition of K^+, immediately ordered mixed-layer domains (Reichweite 1, denoted as R1) consisting of swelling smectitic (1WL; basal spacing of 12.3 Å) and nonswelling illite-like (0WL; basal spacing of 10.0 Å) interlayers are regularly stacked and have been observed by powder X-ray diffraction (PXRD; see Figure 1). Obviously, at low degrees of exchange, the number of collapsed/dehydrated, illite-like interlayers is less than that of the hydrated smectite-type interlayers. The relative amounts of hydrated and collapsed interlayers are expressed by ω_{hyd} and ω_{col}, respectively.

Even at minor degrees of exchange ($\omega_{hyd} > \omega_{col}$), the basal reflections of the Na-Hec end-member were not shifted toward the position of the K-Hec end-member, as might be expected from Méring's law.[37,38] Instead, a new set of basal reflections of the ordered mixed-layer Na:K-Hec is immediately observed, even at partial exchanges as low as 10% K^+. This indicates that, even at the initial stages of exchange, ordered domains seem to be preferentially built, increasing the tendency of forming such regularly interstratified materials. Upon further K^+-exchange, the intensities of the 00*l* series of the Na-Hec end-member gradually vanish, while, correspondingly, the intensities of the 00*l* series of the ordered mixed-layer Na:K-Hec steadily increase. The volume of the ordered mixed-layer domains increases as the exchange progresses, while the homoionic Na-Hec domains vanish to the same extent. The intensity of the d'(001)-superstructure reflex at 22.3 Å is maximized at an addition of 40%−50% K^+, which indicates that $\omega_{hyd} = \omega_{col}$ is approached. Upon further exchange, d'(001) diminishes quickly and is completely gone when 60% K^+ is reached.

The immediate formation of a second domain of regularly interstratified stacks suggests that K^+-exchange does not proceed randomly within a tactoid. It seems that, after a particular interlayer collapses, it acts as a nucleus for the propagation of the ordered domain, which advances in a cooperative manner along the stacking direction. We will return to this point when we discuss the formation mechanism of the ordered domains. Interestingly, the further addition of K^+ beyond $\omega_{hyd} = \omega_{col}$ does not yield a second, pure K-Hec phase in addition to the regularly interstratified domain, but, instead, a surplus of collapsed interlayers ($\omega_{hyd} < \omega_{col}$) is randomly interspersed between the ordered Na:K-Hec domains (see Figure 2d), as indicated by the gradual shift of d'(002) according to Méring's law, until it finally merges into the d(001) of the K-Hec end-member.

The ordered mixed-layer material (R1, $\omega_{hyd} = \omega_{col}$) closely resembles the natural mineral rectorite, which also shows a regularly interstratified sequence of illite- and smectite-like layers. Although experimental evidence is scarce, because of the reasons listed in the Introduction, it is generally accepted that the regular alteration of hydrated and nonhydrated interlayers coincides with alternating pronouncedly different densities of interlayer cations.[39] These regular charge density variations of smectite-type and mica-type interlayer cation densities are, in turn, thought to be the consequence of an ordered stacking of polar lamellae. Each lamella in the stack is identical and contains an aluminum-rich and an aluminum-poor tetrahedral sheet. The up−down alternating of these polar lamellae results in two distinct interlamellar spaces (see Figure 3). The smectite-like interlamellar

(37) Méring, J. *Acta Crystallogr.* **1948**, *2*, 371–377.
(38) Moore, D. M.; Reynolds, R. C.; Duane, M. *X-ray Diffraction and the Identification and Analysis of Clay Minerals*; Oxford University Press: Oxford, U.K., 1997.
(39) Brown, G. *Phil. Trans. R. Soc. London A* **1984**, *311*, 221–240.

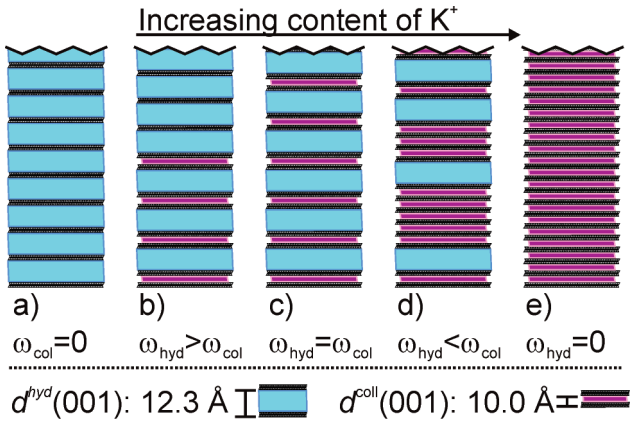

Figure 2. Scheme of the evolution of ordered ($R = 1$) mixed-layer domains with increasing degrees of cation exchange: (a) homocationic, hydrated Na-Hec ($\omega_{col} = 0$); (b) increasing mixed-layer domain added to a still-homocationic Na-Hec domain ($\omega_{hyd} > \omega_{col}$); (c) perfect mixed-layer structure ($\omega_{hyd} = \omega_{col}$); (d) statistical interstratification of residual swelling interlayers ($\omega_{hyd} < \omega_{col}$) within collapsed domains; and (e) completion of the exchange ($\omega_{hyd} = 0$).

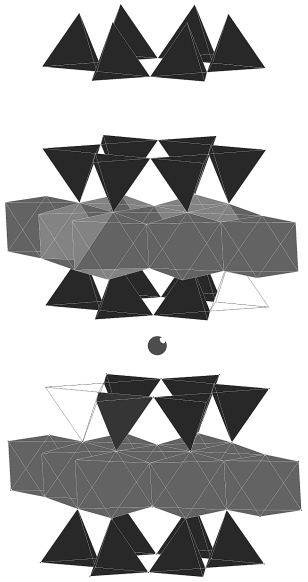

Figure 3. Thermodynamically preferred structural model for the regular interstratification of illite and smectite (rectorite), as proposed by Stixrude and Peacor,[29] based on DFT calculations. Dark tetrahedra represent Si, light tetrahedra represent Al, and dark spheres represent interlayer cations.

space is adjacent to low-charge tetrahedral sheets, and the illite-like one is adjacent to high-charge tetrahedral sheets. Stixrude and Peacor recently proved, with DFT calculations, that this model is energetically favored over alternative models discussed in the literature.[29] According to this model, complete dissolution and neocrystallization of both lamellae and stacked tactoids are the most likely building mechanisms for interstratified materials, because the differences in Al−Si ordering between rectorite and the two end-members of illite and smectite cannot be achieved by low-temperature solid-state diffusion of Al and Si. However, even when one does accept dissolution and neocrystallization as the building mechanism, the driving force for the formation of polar lamellae is unclear, and this situation is even more vague for the oriented alternating stacking.

In the present experiments, we are clearly dealing with symmetric, nonpolar lamellae, as highlighted previously. Solubilities are too low, reaction times are too short, and temperatures are too low to allow any structural changes of the silicate lamellae. Consequently, another simpler and more rapid mechanism must be in action to break symmetry along the stacking direction and to differentiate between two distinct interlamellar spaces in an ordered fashion.

The few incidences in which ordered interstratified materials have been reported in the literature provide a first hint toward this mechanism. Tateyama synthesized $[Na_{0.66}]^{inter}[Mg_{2.70}]^{oct}[Si_{3.95}Al_{0.02}Mg_{0.03}]^{tet}O_{10.06}F_{1.88}$ using a high-temperature solid-state reaction (2 h, 800 °C) by reacting talcum with Na_2SiF_6.[40] Upon a 50% cation exchange by Mg^{2+} and partial drying by heating the sample to 73 °C, superstructure reflections were observed at 22.1 and 11.6 Å, which were explained by the ordered interstratification of hydrated Mg interlayers and collapsed Na interlayers. As already mentioned, Pinnavaia et al.[20−22] described the formation of mixed inorganic−organic ordered interstratifications using a commercial, high-charge lithium hectorite (Corning, Inc.), which was manufactured by a melt synthesis. Finally, regular interstratification is frequently encountered in natural vermiculites.[41] Sawhney suggested that the formation of ordered mixed-layer materials resulted from the density reduction of interlayer cations in the two interlayers adjacent to the collapsed K-interlayers.[42] This would suggest that the alteration of interlayer cation density is achieved solely by reshuffling the interlayer cations while the structure and composition of the silicate lamellae are left unchanged. Moreover, since heterogeneities in charge density are minimized in materials made at high temperatures, and since it is well-known that charge density fluctuations are much less pronounced in vermiculites as compared to smectites,[43] one might hypothesize that it is, indeed, the homogeneity of the layer charge density that is at the core of the formation of ordered mixed-layer materials.

3.2. Proposed New Mechanism for the Formation of Ordered Mixed-layer Materials. A plausible mechanism must answer two questions:

1. Starting from completely hydrated homogeneous Na-Hec, how and what initiates the differentiation into still hydrated and collapsed interlayers?

2. How is the cooperativity along the stacking direction assured? Why is every collapsed layer adjacent to two hydrated layers?

Generally, the regular interstratification could be the product of thermodynamic or kinetic control. Lagaly discussed a mechanism based on a kinetic effect. Starting with a completely collapsed material, he suggested negative cooperativeness, meaning that swelling-induced

(40) Tateyama, H.; Noma, H.; Nishimura, S.; Adachi, Y.; Ooi, M.; Urabe, K. *Clays Clay Miner.* **1998**, *46*, 245–255.
(41) Sawhney, B. L. *Clays Clay Miner.* **1972**, *20*, 93–100.
(42) Sawhney, B. L. *Clays Clay Miner.* **1967**, *15*, 75–84.
(43) Lagaly, G. *Clays Clay Miner.* **1982**, *30*, 215–222.

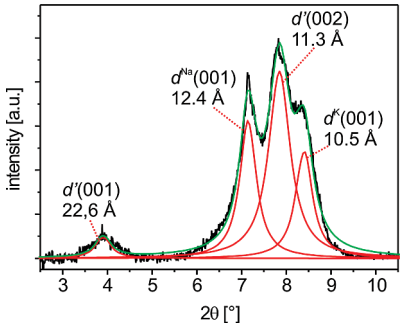

Figure 4. Powder X-ray diffraction (PXRD) pattern after a 6-day "converging" reaction of a 1:1-mixture of homoionic Na-Hec and K-Hec.

deformation of the silicate lamellae will block the two adjacent interlayers.[44] However, we begin with a completely swollen state, so this mechanism cannot explain the ordered collapse of every second interlayer. Nevertheless, a simple experiment was performed to test Lagaly's hypothesis. Equal portions of dry homocationic Na-Hec and completely exchanged K-Hec were combined and immersed in water. Both hectorites were washed excessively before mixing, to ensure that only ionically fixed interlayer Na^+ and K^+ were present. The transformation of the two end-members into an ordered mixed-layer structure by this convergent method is slow, compared to the procedure using Na-Hec and KCl solution. Even after 6 days at 60 °C, the conversion is not close to completion, and three distinct (00*l*)-reflections are observed in the PXRD (see Figure 4) for regular interstratification, and the two end-members are supplied as educts (Na-Hec and K-Hec). Deconvolution of the PXRD pattern gave values of 12.4 Å for Na(001) and 10.5 Å for K(001). These values are shifted to slightly larger values, compared to the end-member homocationic hectorites. In addition, the superstructure reflections of the ordered mixed-layer phase built by the converging process are slightly shifted ($d'(001) = 22.9$ Å and $d'(002) = 11.45$ Å), in comparison to the material obtained by mixing solid Na-Hec with a KCl solution ($d'(001) = 22.6$ Å and $d'(002) = 11.3$ Å). These shifts can be attributed to minor degrees of random interstratifications of the "wrong" basal spacings in all three phases. In any case, these results prove that the formation of the ordered mixed-layer phase is clearly driven by thermodynamics. Apparently, the balance between maximizing the hydration enthalpy of the Na^+ interlayer cations on one side and minimizing the average basal spacings in order to gain the maximum Coulombic interaction in the stacking on the other side produces the interstratification of hydrated and collapsed interlayers as the thermodynamic minimum of these heterocationic materials. Obviously, one would assume that the collapsed and hydrated interlayers are predominantly occupied by K^+ and Na^+ cations, respectively.

As noted previously, the fluorohectorite structures used here are inherently symmetrical, with respect to the

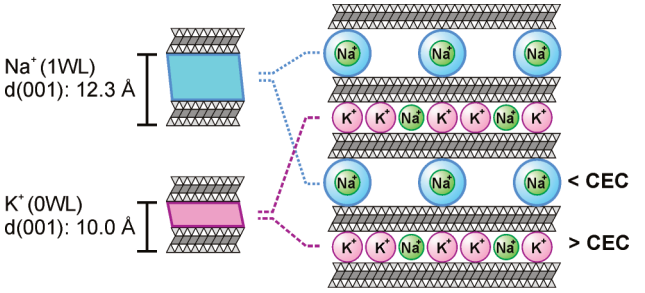

Figure 5. Alternating interlayer cation deficiency and excess as the basis for the formation of ordered mixed hydrated-dehydrated layer structures. Small amounts of Na^+ are trapped inside K^+-rich interlayers. Dehydrated K^+ acts as a pillar, cross-linking the interlamellar space in a defined way, and this fixes the relative position of adjacent silicate lamellae.

charge distribution perpendicular to the lamellae. Therefore, a structural predisposition built into the lamellae, as suggested by Stixrude and Peacor[29] and others, to differentiate between hydrated smectite-like and collapsed illite-like interlayers can be ruled out. Instead, an alternative mechanism must break the symmetry along the stacking direction spontaneously. The mechanism must involve nonpolar lamellae, and it must also explain the cooperativity along the stacking direction, which is required to produce an ordered mixed-layer material. As we will highlight by several experiments, this mechanism is centered at the interlayers. While the charge density of all silicate lamellae is homogeneous throughout the material and does not change upon formation of regular interstratification, the charge density of the interlayers changes from homogeneous to regularly varying from interlayer to interlayer in the stacking direction. While the postulate of polar lamellae requires dissolution and neocrystallization as the building mechanism, our novel mechanism suggests a simple redistribution of exchangeable interlayer cations that is facile and fast and does not require large activation energies. The redistribution of interlayer cations will produce a regularly alternating deviation in the cationic exchange capacity of the interlayers (see Figure 5). The CEC of the collapsed interlayers is higher than the average CEC, while the CEC of the hydrated interlayers will be correspondingly lower. Such regular fluctuations of electron density along the stacking direction are corroborated by PXRD.[39] This mechanism is closely related to the LCECL model introduced by Meier and Nüesch,[45] as well as that suggested by Sawhney[42] for the formation of regular interstratification with vermiculites.

Most importantly, this interlayer-centered reshuffling mechanism can also explain the cooperativity along the stacking direction in a simple way. According to Pauling,[46] the charge balance in an ionic material must be locally realized. In that respect, layered polyanionic materials are a somewhat special case as a first approximation, and the required local charge balance can be equally well-estimated by arranging various proportions

(44) Lagaly, G. *Developments in Ionic Polymers*; Wilson, A. D., Prosser, H. J., Eds.; Elsevier: London, 1986.

(45) Meier, L. P.; Nüesch, R. *J. Colloid Interface Sci.* **1999**, *217*, 77–85.
(46) Pauling, L. *Nature of the Chemical Bond*; Cornell University Press: New York, 1948.

of the counterions above and below the lamella. The symmetrical 50:50 arrangement is only slightly favored over unsymmetrical arrangements (e.g., 60/40), since the lateral repulsion of cations occurs inside the same interlamellar plane. However, the unsymmetrical arrangement might be still thermodynamically preferred, because an excess of interlayer cations in the collapsed/nonswollen interlayers will contribute disproportionally to the Coulombic interaction, while the hydration enthalpy of swollen interlayers is only slightly diminished by lowering the cation concentration. To ensure the local charge balance, each high-charge interlayer must be adjacent to two low-charge interlayers, which neatly explains the R1 ordering. In this way, as corroborated by the formation of ordered domains at comparatively low degrees of exchange, the formation of the first high-charge interlayer acts as a nucleus for the formation of the ordered domain, which then spreads in both directions along the stacking direction. Increased cation density and the low hydration enthalpy of K^+ will induce a lower hydration state for the high-charge interlayers, compared to the low-charge interlayers. In air, the high-charge interlayers completely dehydrate and collapse to a basal spacing of 10 Å. Preliminary in situ PXRD suggest that, in an aqueous suspension, even the high-charge interlayers are still hydrated to *d*-values larger than 12 Å and collapse is only triggered upon drying. This would imply that even the high-charge interlayers are accessible throughout the formation of the ordered mixed-layer structure. Therefore, the relocation of interlayer cations seems to be an equilibrium process at every stage, and defects in the ordered mixed-layer stacking could be repaired.

In summary, this model would break the symmetry by differentiating the two interlamellar spaces adjacent to a particular silicate lamella. While the average concentration of interlamellar cations still matches the charge density of the polyanionic lamellae, the interlamellar space above would show a CEC larger than the average CEC (CEC_{ave}). Conversely, the adjacent interlayers below and above would show CEC < CEC_{ave}. After this differentiation has occurred at one particular spot inside the stack, local charge balance requirements will force this differentiation in a cooperative mode throughout the entire stack.

Straightforward experimental proof of the suggested mechanism would require an analytical method with a spatial resolution of <1 nm, which is not available. Therefore, proof can only be provided by indirect means, which would require some preliminary experiments regarding selectivity and kinetics of ion exchange of the different phases. As mentioned, one would expect the collapsed interlamellar spaces to be predominantly occupied by K^+, while the hydrated areas will be occupied by Na^+.

The driving force for the K^+ exchange is the higher selectivity of K^+, as compared to Na^+.[47] Figure 6 illustrates the relative K^+ adsorption in relationship to the addition of K^+ at an initial K^+ concentration of 20 mM. Up to 50 mol % (relative to the total Na^+), the K^+ exchange is almost quantitative in supporting the high selectivity of the added K^+ for the solid fluorohectorite phase. Beyond this degree of exchange, significant amounts of free K^+ are detected in the aqueous supernatant by atomic absorption spectroscopy (AAS). This means that the released Na^+ cations are able to compete in equilibrium with the residual free K^+ in solution only at higher degrees of exchange, despite the higher selectivity of K^+. At up to 50 mol %, the exchange is literally quantitative and every K^+ available in the solution will replace a Na^+ in the fluorohectorite. According to PXRD, quantitative analysis of the supernatants, and the solid mixed cationic fluorohectorites, the most regularly interstratified material (R1; $\omega_{hyd} = \omega_{col}$) is obtained at 50 mol % exchange. This would initially contradict the suggested mechanism, which requires collapsed interlayers with CEC > CEC_{ave} and hydrated interlayers with CEC < CEC_{ave}. However, note that the proposed nonsymmetrical arrangement of interlayer cations can still be obtained upon the addition of 50 mol % K^+ if the collapsed interlamellar spaces contain residual Na^+ in addition to K^+ (recall Figure 5).

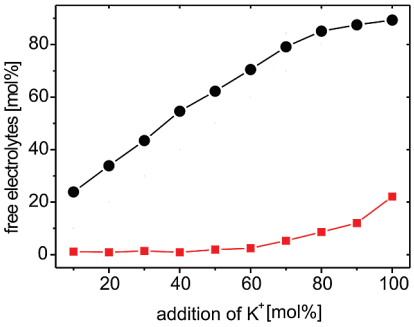

Figure 6. Quantitative analysis of the aqueous supernatant for Na^+ (denoted by solid black circles) and K^+ (denoted by solid red squares) by atomic absorption spectroscopy (AAS). The results are normalized to the total Na^+ content of the freshly synthesized Na-Hec.

As noted previously, chemical analysis with a subnanometer spatial resolution is not available. Therefore, we must rely on local methods to experimentally prove the differentiation of interlamellar spaces and the mixed nature of the collapsed interlayers: selective cation exchange, swelling properties with water (hydrosorption isotherms), and ^{23}Na MAS NMR spectroscopy.

3.3. Selective Cation Exchange. Although the interlamellar reactivity of the collapsed interlayers will not be null, the reactivity of the hydrated interlamellar spaces will be orders of magnitude higher. This can be addressed selectively by fast ion exchange (see Figure 7). Using the highly selective complex cation $[Cu(trien)]^{2+}$, the photometric measurement of the cation exchange capacity,[30,48] which is restricted to the hydrated interlayers, is feasible. When exposing Na-Hec to $[Cu(trien)]^{2+}$, stoichiometric cation exchange is achieved almost instantly and remains constant at a level corresponding to the total CEC

(47) Maes, A.; Cremers, A. *ACS Symp. Ser.* **1986**, *323*, 254–295.

(48) Meier, L. P.; Kahr, G. *Clays Clay Miner.* **1999**, *47*, 386–388.

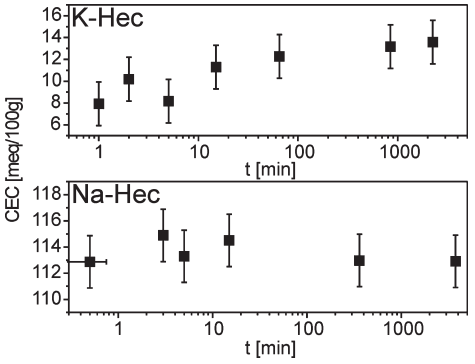

Figure 7. Evolution of the CEC with time for homoionic Na-Hec and K-Hec, respectively. The CEC was determined according the $[Cu(trien)]^{2+}$ method.

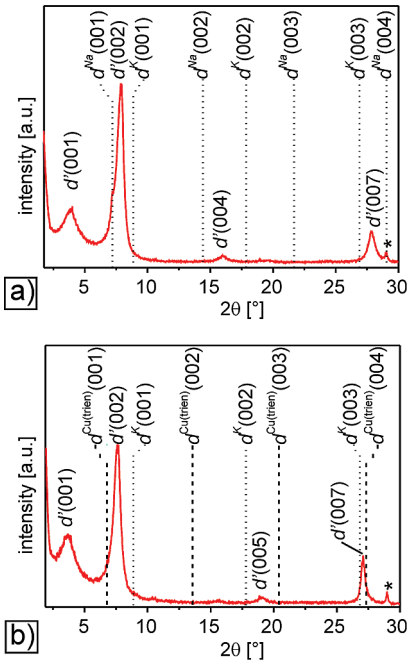

Figure 8. PXRD patterns of (a) regularly interstratified Na:K-Hec, as obtained by 50 mol % addition of K^+ to Na-Hec, and (b) regularly interstratified Cu(trien):K-Hec obtained by exposing Na:K-Hec to $[Cu(trien)]^{2+}$ in slight stoichiometrical excess. The dotted and dashed lines represent the reflex positions of the corresponding purely homocationic hectorites.

(113 mequiv/100 g). Conversely, the corresponding homoionic K-Hec exhibits an initial CEC of 8 mequiv/100 g that is due solely to the outer surfaces. The additional $[Cu(trien)]^{2+}$ is slowly intercalated as time elapses, indicating a high activation energy for the exchange into interlamellar spaces due to the limited intracrystalline reactivity of the collapsed K^+ interlayers.

PXRD measurements provide additional evidence for the feasibility of selective cation exchange of the hydrated interlayers. Regularly interstratified Na:K-Hec can be used as a starting material to create functionalized interstratified fluorohectorites. Ordered mixed-layer Na:K-Hec (see Figure 8a) was exposed to $[Cu(trien)]^{2+}$ in slight stoichiometrical excess to model this reaction. Fast cation exchange can be restricted to the swelling interlayers, allowing these hydrated interlayers to be selectively targeted (exchange of Na^+ versus $[Cu(trien)]^{2+}$) while maintaining the regular interstratification pattern (see Figure 8 b).

The regular interstratification (R1, $\omega_{hyd} = \omega_{col}$) shown in Figure 8a is formed by the addition of 50 mol % of K^+ to Na-Hec. A detailed look at the PXRD patterns reveals that the coefficient of variation of the (00*l*) series (CV) is low (0.83%), but slightly exceeds the 0.75% limit defined by Bailey[49] for regular interstratified materials (see Table S1 in the Supporting Information). Additionally, the superstructure reflection $d'(001)$ shows a higher full width at half maximum (FWHM) value of 0.91°, in comparison to the higher-order $d'(00l)$ reflections, which range from 0.65° and 0.73°. Figure 8b represents the PXRD pattern of the Cu(trien):K-Hec that was prepared from the Na:K-Hec. The observed $d'(001)$ value of the Cu(trien):K-Hec (23.3 Å) is in good agreement with expectations. The sum of the basal spacings of the end-members is 23.3 Å, (Cu(trien)-Hec: $d(001)$ = 13.0 Å and K-Hec $d(001)$ = 10.0 Å). Despite the high selectivity of $[Cu(trien)]^{2+}$ for intercalation, the collapsed interlayers apparently did not undergo cation exchange, and the regularly interstratified character was successfully transformed. The CV of the (00*l*) series after the selective cation exchange becomes even less (0.5%) than that in the starting material (see Table S2 in the Supporting Information).

On the basis of this selective ion exchange of hydrated interlayers, a first proof of the proposed mechanism can now be presented. The CECs of the hydrated interlayers determined by selective cation exchange with $[Cu(trien)]^{2+}$ as a function of the degree of K^+ exchange were compared with the analysis results from AAS for Na^+ and K^+ of these mixed cation fluorohectorite solids. As indicated by the selectivity of the cation exchange (recall Figure 6), up to 50 mol % Na and K contents of the fluorohectorites determined by AAS change linearly and in a reciprocal manner. The sum of Na and K at each degree of exchange corresponds to the total Na content of the pristine Na-Hec. At higher portions of added K^+, the curves flatten in analogy to the previously presented selectivity results. It is important to note that, when comparing the total CEC with the total amount of Na^+ in the solid phase of the homocationic Na-Hec, an offset of ~6 mmol/100 g was observed. The source of this nonexchangeable Na^+ can be attributed to the trace impurity protoamphibole (compare Figure 1 and Figure S1 in the Supporting Information).

It is interesting that the amount of exchangeable Na^+ measured by selective cation exchange with $[Cu(trien)]^{2+}$ increasingly deviates from the total Na content determined by AAS as the K^+ exchange progresses (see Figure 9).

At 50 mol % K^+, the PXRD pattern suggests a regular interstratification with $\omega_{hyd} = \omega_{col}$, and the difference between both Na values is ~12 mmol/100 g. Since the CEC of the hydrated interlayers is significantly less than 50% of the initial CEC (35 mequiv/100 g, compared to 97 mequiv/100 g, respectively), we conclude that the

(49) Bailey, S. W. *Am. Mineral.* **1982**, *67*, 394–398.

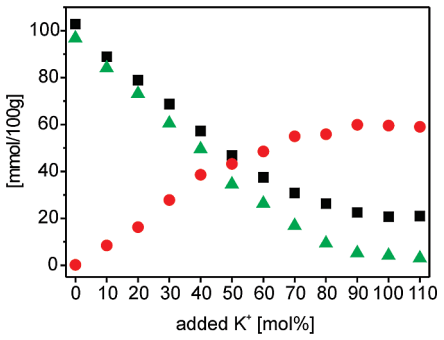

Figure 9. Quantitative determination of the interlayer cations (Na^+ (solid black square) and K^+ (solid red circle)) of mixed-cation fluorohectorites by AAS, in comparison with the CEC (denoted by solid green triangles) of hydrated interlayers, as determined by selective cation exchange with $[Cu(trien)]^{2+}$, as a function of the degree of K^+ exchange.

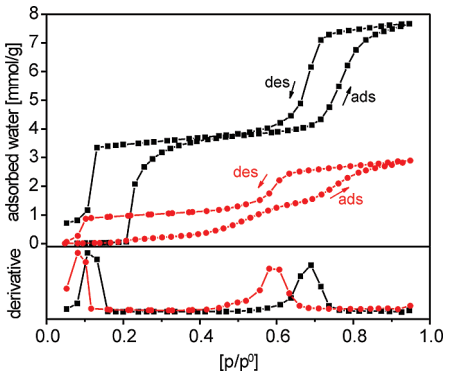

Figure 10. Hydrosorption isotherms (above) of homocationic Na-Hec (denoted by solid black squares) and mixed-layer Na:K-Hec (denoted by solid red circles) taken at 25 °C. The derivatives of both desorption curves (beneath) were normalized for clarity.

hydrated 12.3-Å layers possess ~28% less exchangeable cations than the pristine Na-Hec. This rough estimate does not take into account the gradual change in molar weight that occurs as the cations are replaced. Accounting for this change of molar weight, the hydrated interlayer charge was reduced by 18%. These results suggest that a significant amount of Na^+ was trapped in the illite-like interlayers when these interlamellar spaces collapsed. As indicated in Figure 5, the total cation content of the collapsed interlayers seems to be higher than the average CEC, while the cation content of the hydrated interlayers must be correspondingly lower than the average CEC.

Further evidence for the trapping of some Na^+ cations in the collapsed interlayers is the fact that, even through the addition of excess K^+, the total exchange of Na^+ is not possible. At 110 mol % K^+, significant amounts of Na^+ remain in the fluorohectorite, while the CEC converges to zero.

3.4. Swelling Properties. The swelling of clays is strongly dependent on the interplay of the hydration enthalpy of the interlayer cations and the charge density of the interlamellar space.[50,51] Therefore, the hydrosorption isotherms represent a very sensitive measure of any changes to the composition of the interlamellar space. For the interstratified material, the method is, of course, selective only to the hydrated/swelling interlayers. If the composition of the swelling interlayers does not change upon partial K^+ exchange to form a mixed-layer structure, we would expect the same shape of the hydrosorption isotherm as for the pristine Na-Hec material, except that the amount of the total adsorbed water would differ by a factor of 2.

As expected, the hydrosorption isotherms shown in Figure 10 of the mixed-layer Na:K-Hec show a significant decrease in the total amount of water adsorbed, compared to the homocationic Na-Hec. A comparison of both desorption curves at a relative water vapor pressure of 0.8 shows that the bihydrated (2WL) Na-Hec adsorbed 7.49 mmol/g water, whereas the Na:K-Hec adsorbed considerably less than one-half of that amount (2.74 mmol/g water). In relation to the CEC values, the Na-Hec contains 7.74 water molecules per exchangeable cation, and Na:K-Hec contains 7.93 water molecules per exchangeable cation. If a constant amount of water molecules per interlayer cation is assumed, then the calculated cation density of the hydrated layers of the Na:K-Hec decreased by 27%, compared to the Na-Hec (see the Supporting Information for details of the calculation). At a relative water vapor pressure of 0.4, the relative amount of water per exchangeable cation is 3.8 for Na-Hec and 3.2 for Na:K-Hec. However, shifts and shape changes are the more interesting features of the hydrosorption isotherms. For illustrative purposes, the differences are highlighted by comparing the derivatives of both desorption curves (see bottom portion of Figure 10). The desorption of the mixed-layer hectorite was clearly shifted toward a lower partial pressure (p/p_0) of water. This indicates a decrease in the layer charge since various reports[50,52,53] have stated that a decrease in the layer charge increases the affinity to hydrated states. In other words, the lower the layer charge of a smectite, the more hygroscopic it is, and, thus, the desorption curve must be shifted to lower values of p/p_0. In summary, the amounts of water adsorbed, as well as the observed shifts in partial pressure at which desorption occurs, both support the idea of a reduced interlayer cation concentration being required for the proposed mechanism.

3.5. ^{23}Na MAS NMR Spectroscopy. The proposed mechanism postulates two Na^+ sites (recall Figure 5). One is trapped in the collapsed, predominantly K^+-occupied, high-charge interlayers, and one is in the low-charge, swelling, predominantly Na^+-occupied interlayers. ^{23}Na MAS NMR spectroscopy is sensitive to the local environment and will not only be influenced by the hydration, but also by different planar defects in the stacking of adjacent silicate lamellae. For instance, going from a 1M, mica-type stacking, with hexagonal cavities formed by the basal O atoms being arranged opposite from each other,

(50) Laird, D. A. *Appl. Clay Sci.* **2006**, *34*, 74–87.
(51) Salles, F.; Devautour-Vinot, S.; Bildstein, O.; Jullien, M.; Maurin, G.; Giuntini, J. C.; Douillard, J. M.; Damme, H. V. *J. Phys. Chem. C* **2008**, *112*, 14001–14009.
(52) Slade, P. G.; Quirk, J. P.; Norrish, K. *Clays Clay Miner.* **1991**, *39*, 234–238.
(53) Teppen, B. J.; Miller, D. M. *Soil Sci. Soc. Am. J.* **2006**, *70*, 31–40.

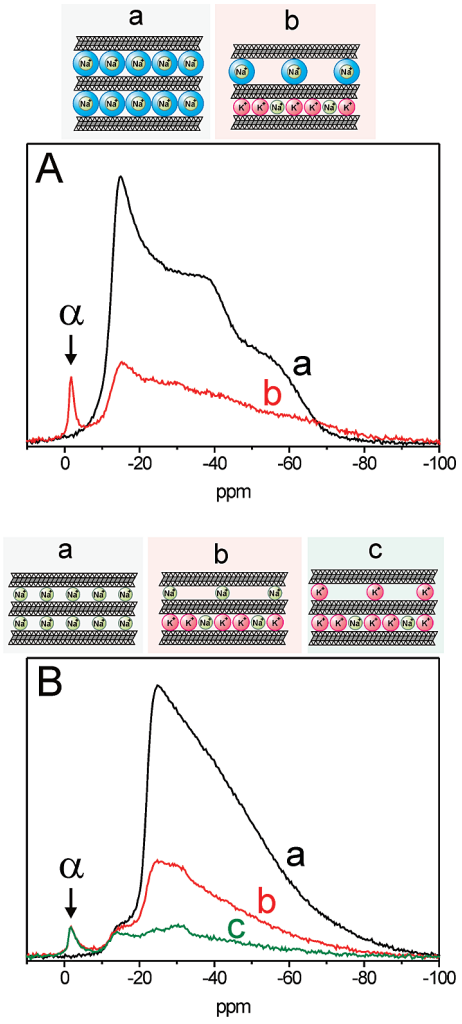

Figure 11. ^{23}Na SS NMR spectra of (a) Na-Hec, (b) the ordered mixed-layer Na:K-Hec, and (c) K-Hec* at 45% (panel A) and 0% RH (panel B). Upon the collapse by partial K^+ exchange, a sharp Na signal (α) appears.

to a $\pm b/3$ translationally disordered stacking, the coordination number of the interlayer cation is reduced from 6 + 6 to 6 + 3. Since K^+ is larger than Na^+ and fits perfectly into the mentioned hexagonal cavities, it is well-known that, upon K^+ exchange, the translational disorder is diminished and further 1M-type stacking results. As indicated by the shape of the *hk* bands, the stacking in the hydrated pristine Na-Hec is turbostratic, meaning that arbitrary translational and/or rotational disorder occurs. Consequently, it is expected that ^{23}Na MAS NMR spectra of the Na sites in the collapsed high-charge interlayers will be affected by both dehydration and improved stacking order.

The sodium population in the pure Na-Hec measured at 45% and at 0% RH causes a broad signal dominated by the quadrupolar interaction with a coupling constant (QCC) that is greater than 3.0 MHz (estimated from the line width of the black lines in Figure 11). This is generated by the highly asymmetric environment of the sodium nuclei, which is due to turbostratic disorder of the Na-Hec. The more-distinct features of the ^{23}Na spectrum of the Na-Hec measured at 45% RH (Figure 11A, black line), compared to that collected at 0% RH (Figure 11B, black line) are a consequence of the local mobility of the

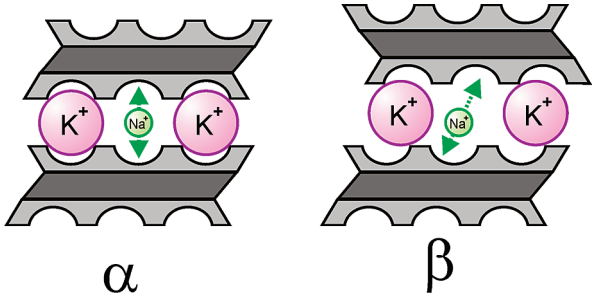

Figure 12. Proposed schematic of trapped sodium: (α) sandwiched, symmetric, mica-like sodium environment and (*β*) disordered, sodium environment.

Na^+ ions at 45% RH, which are surrounded by a water layer. This mobility causes average small-amplitude layer shifts and rotations and, thus, reduces the influence of the spectral shape on the disorder of the surrounding chemical to a certain extent.

The ^{23}Na spectra of the regularly interstratified material (Figure 11, red line) possess a shape similar to that of Na-Hec (Figure 11, black line) between −15 ppm and −80 ppm for both RHs. This resonance is caused by Na^+ ions in a highly disordered environment, which supports the presence of swelling layers occupied mainly by Na^+ cations. Moreover, a second, much-sharper signal at ∼0 ppm is visible in the spectra of the K:Na-Hec (Figure 11, red lines). We will henceforth refer to this as signal α. Since the mobility of the trapped Na is expected to be very limited, the small quadrupolar coupling is surprising at first glance. However, as mentioned previously, the size of the K^+ ions allows them to fit perfectly into the hexagonal cavities of the surface of the lamellae, triggering an ordered mica-type stacking (Figure 12α). The resulting 6 + 6 coordination exhibits a higher degree of symmetry around the trapped Na^+, which again leads to a small quadrupolar interaction and thus a sharp ^{23}Na MAS signal. This statement is supported by quantum mechanical calculations applied in the CASTEP code (for details, see the Experimental Methods section). The calculated QCC of 0.35 MHz is in good agreement with the experimentally observed value of 0.5 MHz (line-shape analyses) and, indeed, is too small to dominate the line shape in the MAS experiments. Consequently, we assign this sharp signal α to trapped Na^+ ions in symmetric cavities created by a mica-type stacking. Similar sharp ^{23}Na MAS signals have been reported in the literature for swelling fluoromica[40,54,55] and have been attributed to the nonexchangeable part of the Na interlayer cations.

The ^{23}Na spectrum acquired for the K-Hec* (trace c in Figure 11 B) exhibits, in addition to the α signal, a very broad signal ranging from −15 ppm to approximately −80 ppm that is attributed to a trace impurity of protoamphibole.[56] However, it cannot be ruled out that

(54) Soma, M.; Tanaka, A.; Seyama, H.; Hayashi, S.; Hayamizu, K. *Clay Sci.* **1990**, *8*, 1–8.
(55) Laperche, V.; Lambert, J. F.; Prost, R.; Fripiat, J. J. *J. Phys. Chem.* **1990**, *94*, 8821–8831.
(56) Delevoye, L.; Liu, S. X.; Welch, M. D.; Fernandez, C.; Amoureux, J. P.; Klinowski, J. *J. Chem. Soc. Faraday Trans.* **1997**, *93*, 2591–2595.

additional Na sites related to the fluorohectorite phase are superimposed on this protoamphibole signal. These trapped Na sites might be located in a less-symmetric environment, because of slight and rare translational disorders (see Figure 12, β).

In summary, the NMR data clearly support the proposed mechanism by verifying the existence of trapped Na^+ in the collapsed interlayers of the ordered mixed-layer material. Moreover, the small quadrupolar coupling observed indicates that these Na^+ reside in a mica-like environment.

Conclusion

Ordered mixed-layer materials were obtained spontaneously from a Na-fluorohectorite. The addition of K^+ induced a nonreversible collapse of every second interlayer (K:Na-Hec), which resulted in a regular sequence of hydrated ($d(001)$ = 12.3 Å) and dehydrated ($d(001)$ = 10.0 Å) layers. We proposed a simple novel mechanism that is centered at the interlayers and does not require polar lamellae. Upon formation of the regular interstratification, the charge density of the interlayers changes from homogeneous to alternating interlayer to interlayer in the stacking direction. This simple redistribution of exchangeable interlayer cations is facile and fast. The cation exchange capacity (CEC) of the collapsed interlayers is higher than the average CEC, while the CEC of the hydrated interlayers will be correspondingly lower. The proposed mechanism was experimentally verified by three independent experiments that are sensitive to either swelling or collapsed interlayers: selective cation exchange, hydrosorption isotherms, and ^{23}Na MAS NMR spectroscopy.

Most importantly, this mechanism suggests that the formation of regularly interstratified materials is not limited to K:Na-Hec materials. In this work, we show that selective functionalization can be used to produce Cu(trien):K-Hec. It is expected that the formation of ordered mixed-layer materials will be generally applicable whenever a situation arises where, in a heterocationic sample, the dense packing of a bulky cation is unable to satisfy the average charge density in a monolayer, and, consequently, the local charge balance will be accomplished by surrounding this layer by two interlayers occupied by a less bulky cation.

With these regular interstratified materials, two distinct nanoreactors separated by a 1-nm-thick insulating lamellae are arranged in a regular manner, which offers unique possibilities for electronic or energetic communication between the two adjacent reaction spaces.

Acknowledgment. We thank the Deutsche Forschungsgemeinschaft (SFB 840) for financial support.

Supporting Information Available: PXRD patterns of Na-Hec and K-Hec, tables with additional data of FWHM and *d*-values for Figures 8a and 8b. Furthermore, a short explanation for the calculation of the layer charge density in section 3.1 is provided. This information is available free of charge via the Internet at http://pubs.acs.org/.